

# *Shaft Power Measurement and Error Analysis Based on Strain Gauges*

Lili Lin<sup>1</sup>, Feng Xu<sup>1</sup>, Jinghao Zhang<sup>1</sup>, He Huang<sup>2</sup>

<sup>1</sup>Ningbo Polytechnic, Ningbo, Zhejiang 315000, China

<sup>2</sup>CSSC 711 Research Institute, Shanghai 200090, China

**Keywords:** Shaft power meter; Strain gauges; Torque; Error analysis

**Abstract:** With the increasing demand for industrial automation and intelligence, shaft power measurement technology, as a key parameter detection method in fields such as ships and wind power, is gradually developing towards high precision and non-contact direction. This article is based on strain gauges, electromagnetic sensing, and wireless communication technology, and designs and develops a non-contact shaft power measuring instrument. Combining experimental verification and theoretical analysis, the measurement principles of speed, torque, and thrust are discussed, and the measurement errors are analyzed in detail, providing a basis for the widespread application of shaft power meters.

## 1. Introduction

In the modern industrial field, shaft power is a key parameter for measuring the operating status and performance of rotating machinery equipment. Its accurate measurement is of great significance for the efficient operation, fault diagnosis, and energy management of the equipment. For example, in the shipbuilding industry, accurate measurement of shaft power can help ship operators timely understand the working status of the ship's propulsion system, optimize the ship's navigation performance, and reduce fuel consumption. Meanwhile, in the field of wind power generation, by accurately measuring the power of the wind turbine main shaft, the operational efficiency of the wind power generation system can be effectively evaluated, providing a basis for equipment maintenance and upgrading<sup>[1]</sup>.

Traditional shaft power measurement often uses contact measurement methods, such as torque sensor measurement. This method requires direct contact between the sensor and the measured shaft, and calculates the shaft power by measuring the strain generated by the shaft under torque<sup>[2]</sup>. Although contact measurement technology can meet conventional measurement needs to some extent, its limitations are becoming increasingly prominent as industrial production develops towards high speed, high precision, and high reliability. The contact measurement method has the problem of inconvenient installation and maintenance<sup>[3]</sup>. Due to the need for direct contact with the tested axis, during the installation process, not only does the equipment need to be stopped and

disassembled, but also the installation position needs to be precise, which undoubtedly increases the difficulty and time cost of installation. Moreover, long-term contact between sensors and shafts during equipment operation can lead to wear and tear, requiring regular maintenance and replacement, which also affects the normal operation time of the equipment<sup>[4]</sup>. Contact measurement is also susceptible to environmental factors such as high temperature, humidity, corrosive gases, etc. These factors can lead to a decrease in sensor performance, measurement accuracy, and even damage to the sensor, thereby affecting the accuracy and reliability of measurement results<sup>[5]</sup>.

From the perspective of measurement accuracy, non-contact measurement technology can effectively avoid the influence of factors such as wear and installation errors caused by the contact between the sensor and the measured shaft in contact measurement, thereby achieving higher precision shaft power measurement<sup>[6]</sup>. High precision measurement results can provide more accurate data support for the performance evaluation and optimization of equipment, helping to improve the operational efficiency and reliability of the equipment<sup>[7]</sup>. From the perspective of industry technological progress, the development of shaft power meters based on non-contact measurement technology will promote innovation and development of shaft power measurement technology, providing more advanced technical means for equipment monitoring and control in the industrial field. This not only helps to improve the automation and intelligence level of related industries, but also promotes technological upgrading and industrial development in the entire industrial sector, pushing industrial production towards a more efficient, intelligent, and green direction<sup>[8]</sup>.

## 2. Principle of shaft power measurement

For a rotating shaft, the transmitted power is<sup>[9]</sup>:

$$P = \frac{T_q \times 2\pi n}{60}$$

Among them,  $P$  ——shaft power, kW

$T_q$  ——shaft torque, kNm

$n$  ——shaft revolution, rev/min

Therefore, by accurately measuring the torque and revolution values, the power value can be calculated.

### 2.1.Revolution measurement

Rotational speed is the number of times an object in circular motion completes a circle around its center per unit time<sup>[10]</sup>. There are two methods for measuring rotational speed: frequency measurement and cycle measurement. Cycle measurement (Also called T-method)is a pulse time counting method that calculates rotational speed by measuring the time interval between two pulses in the encoder. In practical use, the time interval between two pulses of the encoder is calculated by the number of high-frequency clock pulses<sup>[11]</sup>.

### 2.2.Torque measurement

The torque value can be measured by strain gauges<sup>[12]</sup>. When the spindle transmits torque, the strain gauges will deform synchronously, as shown in Figure 1.

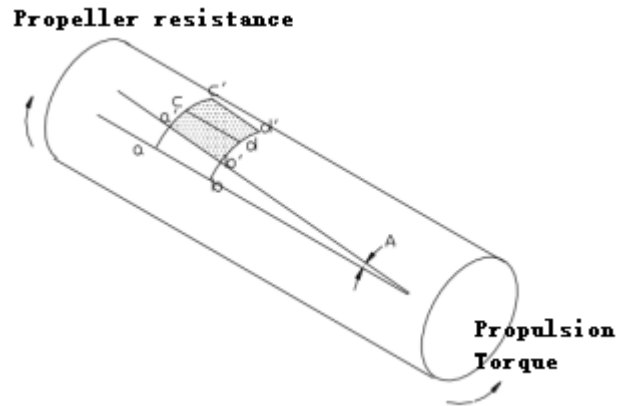


Figure 1. Schematic diagram of torque measurement using strain gauges

The relationship between the original strain value generated by the strain gauge ( mV/V )and the shaft torque( KNm) is as follows:

$$mV/V = \frac{T_q \times 16 \times GF \times (1 + \sigma)}{(D_o - D_i)^3 \times \pi \times E}$$

Among them, mV/V ——original strain value, dimensionless

$T_q$  ——shaft torque, KNm

$GF$  ——strain coefficient,dimensionless

$\sigma$  ——Poisson's ratio

$D_o$  ——shaft outer diameter,unit:m

$D_i$  ——shaft inner diameter,unit:m

$E$  ——Young's modulus, unit: MPa

For example, the calibration calculation parameters for the main shaft torque of a certain ship are as shown in Table 1:

Table 1. A ship shaft parameters

No	parameter	value	unit
1	Shaft outer diameter	0.2	m
2	Shaft inner diameter	0	m
3	Maximum allowable torque of the spindle	200	KNm
4	Maximum allowable thrust of the spindle	200	KN
5	Young's modulus	207000	Mpa
6	Poisson's ratio	0.285	/
7	strain coefficient	2.09	/

Substitute the above parameters into the formula and calculate to obtain

$$mV/V = 1.65192066826956.$$

That means, the strain gauge value 1.65192066826956 corresponding to the torque value 200kNm.Linearizing the corresponding relationship yields serialized values:

mV/V	0.1	0.2	0.3	0.4	0.5	0.6
kNm	12.107	24.214	36.321	48.428	60.536	72.643
mV/V	0.7	0.8	0.9	1.0	1.5	2.0
kNm	84.750	96.857	108.964	121.071	181.607	242.142

If the maximum allowable torque of different ship spindles vary, the linearization relationship will also change.

If the current spindle is unloaded and the mV/V value is not 0, it may be 0.121, then a certain torque value will be displayed and the current value needs to be set to zero.

### 2.3. Thrust measurement

When the spindle is transmitting thrust, the strain gauges will deform synchronously, and the thrust value can be measured by the strain gauge. The relationship between the original strain value generated by the strain gauge (mV/V) and the axial thrust (KNm) is as follows:

$$T_u = \frac{2 \times (\text{mV/V}) \times \pi \times E \times \left( (D_o / 2)^2 - (D_i / 2)^2 \right)}{GF \times (1 + \sigma)}$$

Among them, mV/V — original strain value, dimensionless

$T_u$  — shaft thrust, KN

$GF$  — strain coefficient, dimensionless

$\sigma$  — Poisson's ratio

$D_o$  — shaft outer diameter, unit: m

$D_i$  — shaft inner diameter, unit: m

$E$  — Young's modulus, unit: MPa

Substitute the parameters from Table 1 into the formula and calculate to obtain:

$$\text{mV/V} = 0.041298016706739$$

That means, the strain gauge value 0.041298016706739 corresponding to the thrust value 200kN.

Linearizing the corresponding relationship yields serialized values:

mV/V	0.1	0.2	0.3	0.4	0.5	0.6
kN	0.484285	0.968570	1.452854	1.937139	2.421424	2.905709
mV/V	0.7	0.8	0.9	1.0	1.5	2.0
kN	3.389993	3.874278	4.358563	4.842848	7.264271	9.685695

## 3. Measure Error Analysis

### 3.1. Speed error rate

Assuming the frequency of the high-frequency pulse is  $f_0$ , the time interval between two pulses  $T_t = M_2 / f_0$ , the number of pulses output by the encoder per revolution  $Z$  (with only one Hall sensor and a shaft power meter  $Z=1$ ), as shown in figure 2 and the motor speed can be expressed as:

$$n = \frac{60}{Z \times T_t} = \frac{60 \times f_0}{Z \times M_2}$$

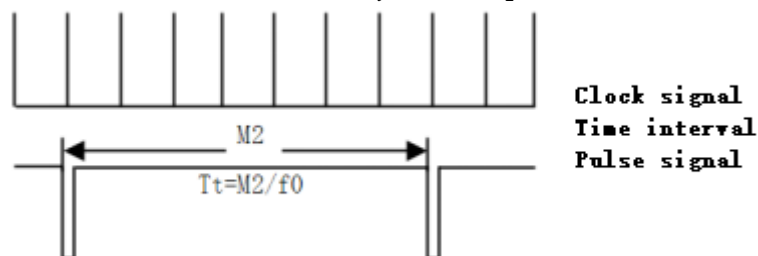


Figure 2. Principle of speed measurement

When the speed changes, assuming that the number of high-frequency clock pulses changes from  $M_2$  to  $M_2-1$ , the resolution of T-method speed measurement can be calculated as:

$$Q = \frac{60 \times f_0}{Z \times (M_2 - 1)} - \frac{60 \times f_0}{Z \times M_2} = \frac{60 \times f_0}{Z \times M_2 (M_2 - 1)}$$

By substituting the rotational speed  $n$  into the above equation, we can derive:

$$Q = \frac{Z \times n^2}{60 \times f_0 - Z \times n}$$

It can be seen that the resolution  $Q$  of T-method speed measurement is related to the rotational speed. The lower the rotational speed, the smaller the  $Q$  value, and the stronger the resolution ability. The maximum error rate of T-method speed measurement can be calculated as follows:

$$\delta_{\max} = \frac{\frac{60 \times f_0}{Z \times (M_2 - 1)} - \frac{60 \times f_0}{Z \times M_2}}{\frac{60 \times f_0}{Z \times M_2}} \times 100\% = \frac{1}{M_2 - 1} \times 100\%$$

For the main shaft of a ship, typical values include:  $f_0=1953.125\text{Hz}$ ,  $0 \leq n < 1000\text{r/min}$ ,  $2 < M_2 < 65535$ .

So the range of speed error rate is  $0.0015\% < \delta_{\max} < 0.086\%$ .

### 3.2. Analysis of Torque and Thrust Error

Full-bridge circuit as show in Figure 3:

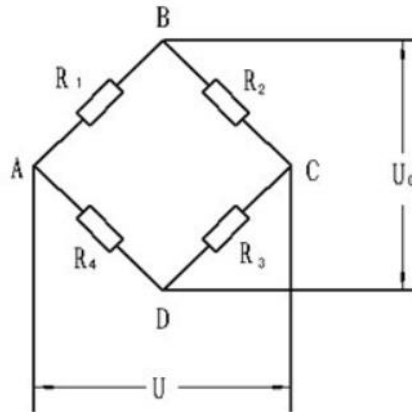


Figure 3. Principle of full-bridge circuit

From the schematic diagram of the full bridge strain gauge circuit, it has:

$$U_o = U_{AB} - U_{AD}$$

$$U_{AB} = \frac{R_1}{R_1 + R_2} U$$

$$U_{AD} = \frac{R_4}{R_3 + R_4} U$$

Substituting the  $U_{AB}$   $U_{AD}$  formulas into the  $U_o$  formula yields:

$$U_o = U_{AB} - U_{AD} = \frac{R_1}{R_1 + R_2} U - \frac{R_4}{R_3 + R_4} U = \frac{R_1 R_3 - R_2 R_4}{(R_1 + R_2)(R_3 + R_4)} U$$

From the above equation, it can be seen that when there is an excitation voltage (i.e.  $U \neq 0$ ), the

condition for  $U_o=0$  is  $R_1R_3=R_2R_4$ , and when the four resistors are equal ( $R_1=R_3=R_2=R_4=R$ ), it is equal arm resistance. When the resistance values of the four resistors change, such as when there are four strain gauges on the bridge arm to measure torque, etc. The output voltage formula is as follows:

$$U_o = \frac{(R + \Delta R_1)(R + \Delta R_3) - (R + \Delta R_2)(R + \Delta R_4)}{(2R + \Delta R_1 + \Delta R_2) (2R + \Delta R_3 + \Delta R_4)} U$$

Due to  $\Delta R_i \ll R$  and omitting higher-order terms in the above equation. The formula is linearized to obtain:

$$U_o' = \frac{1}{4} \left( \frac{\Delta R_1}{R} - \frac{\Delta R_2}{R} + \frac{\Delta R_3}{R} - \frac{\Delta R_4}{R} \right) U$$

The above formula is a linear expression with nonlinear errors. The calculation of nonlinear errors is as follows:

$$\gamma = \left| \frac{U_o - U_o'}{U_o'} \right| * 100\% = \frac{1}{2} \left( \frac{\Delta R_1}{R} + \frac{\Delta R_2}{R} + \frac{\Delta R_3}{R} + \frac{\Delta R_4}{R} \right) U$$

So, as long as four strain gauges are connected to the full bridge circuit, the change direction of  $R_1$  and  $R_3$  resistance values is the same, and the change direction and magnitude of  $R_2$  and  $R_4$  resistance values are the same. Then:

$$U_o = \left( \frac{\Delta R}{R} \right) U \quad \gamma = 0$$

## 4. Shaft power meter design

### 4.1. Composition and parameters

The shaft power composition diagram designed based on the above principle is shown in Figure 4. It includes 5 main parts.

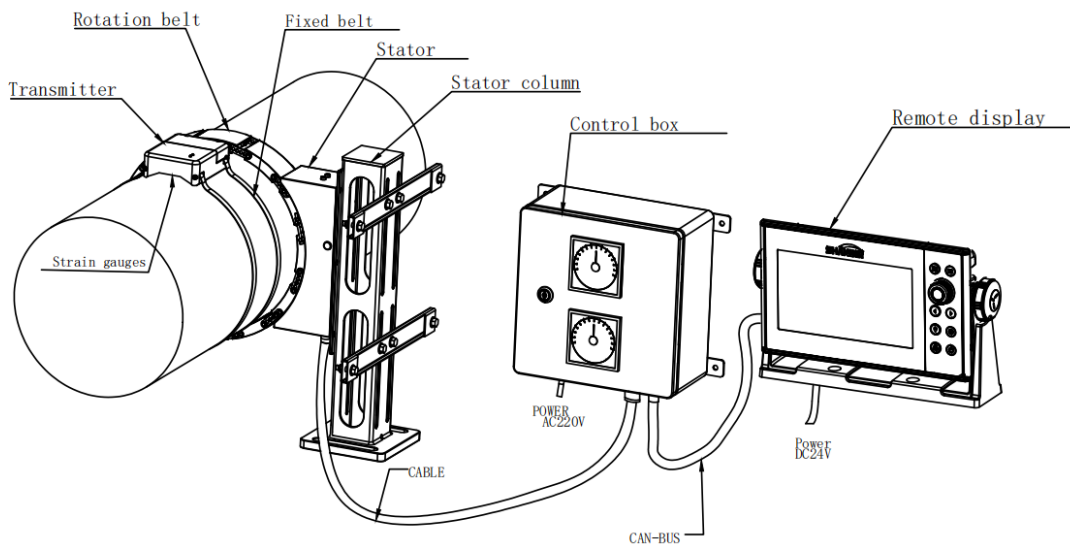


Figure 4. Shaft power composition diagram

1) Transmitter: The function is to collect axial strain signals. The transmitter is installed on the

shaft through a clamp, with a full bridge strain gauge inside. The signal output from the small changes in the shaft shape and position is obtained through an AD sampling circuit, and the data is sent to the stator through a 2.4GHz wireless signal.

2)Rotation belt: The function is to provide power to the transmitter and provide speed pulse signals. The rotor belt adopts a modular design, consisting of multiple identical rotor modules, the number of which is calculated according to the diameter of the main shaft. The rotor modules are connected by independent connecting rod components, equipped with magnetic induction coils inside, and sealed with glue. One of the rotor modules is also equipped with permanent magnets to provide pulse signals for speed detection.

3)Stator: The function is to receive the 2.4GHz signal from the transmitter, provide excitation for the rotor belt, detect the spindle speed, and preprocess the data to send it to the local control box via RS485 signal. The stator must maintain a certain gap with the rotor belt to ensure stable power transmission of wireless power supply.

4)Control box: The function is to display, set, store, and process local torque, speed, and power data. The machine side control box can provide multiple analog and digital signal outputs to other ship performance monitoring systems or power management systems.

5)Remote box: The function is to display historical data, perform parameter statistics, and output reports in the control room, central control room, and other locations. The remote display provides short-term (24-hour) or long-term (5-year) axis power parameter queries in the form of icon curves, and calculates cumulative values. A voyage report can also be issued to calculate the energy transmitted by the main axis and the number of rotations during this voyage, providing a basis for maintenance decisions.

The main technical parameters of shaft power meter are shown in Table 2.

*Table 2. Main technical parameters of shaft power meter*

Applicability	Shaft Dia. Range	150~1150mm		
	Max. Rev.	1000rpm		
	Shaft material	alloy steel		
	Installation space	Axial installation width300mm; Space between stator column and main shaft300mm		
	Max. Shaft num.	3 shafts		
Working principle	Torque sensor	Full-bridge strain gauge		
	Rev. sensor	magnetic induction		
	Power supply	non-contact		
	Data transmission	2.4GHz encryption		
Performance	Power	110-230VAC,24VDC		
	Display	7-inch touch screen; Real time power, torque, and speed, with a sampling period that can be set from 1 second to 15 minutes; Accumulated output energy of the host kWh; The average power of the host is MW;		
	Accuracy	Torque 0.5%	Rev. 0.5%	Power 0.5%
	Send Frequency	10Hz		
Output	analog signal	4~20mA *4		
	RS232/422	2 channels		
Installation	Protection	IP65		
	Air gap	Radial diameter of rotor stator 5-10mm, lateral $\pm$ 8mm		
Environment	Work temperature	5~55°C		
	Storage temperature	-25~70°C		

## 4.2. Test

The product has completed the development of a test prototype, which is installed on a self-developed rotating platform and works normally. The prototype photo is shown in figure 5.

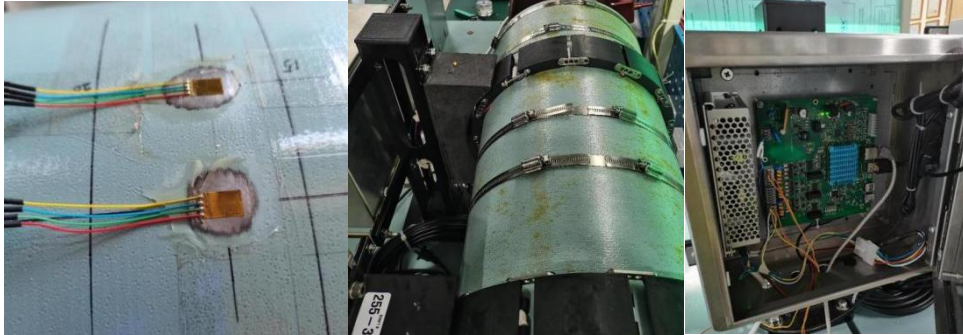


*Figure 5. Shaft power meter picture*

The product of this project has undergone bench simulation comparison tests and actual ship installation tests. The bench simulation comparison tests were conducted on a spindle rotating bench with a spindle diameter of 300mm, which can accurately control the spindle speed through a servo motor system. The main purpose is to verify the working principle of the shaft power meter system and the accuracy of speed measurement<sup>[13]</sup>.

The actual ship installation test was conducted on a 126m long sand transport ship, and participated in berthing tests and trial voyage tests, mainly to verify the performance of the shaft power meter system in actual ship operation and the accuracy of torque measurement. The actual ship test photos are shown in Figure 6.



*Figure 6. Shaft power meter installed in a 126m ship*

Through bench testing and actual ship installation testing, it can be found that the shaft power meter designed in this article has achieved the functions and parameters listed in Table 2, which can meet the application requirements.



## 5. Summarize

Although significant achievements have been made in the development of shaft power meters based on non-contact measurement technology in this study, there are still some shortcomings that need to be further improved and perfected in future research.

In terms of measurement accuracy, although the current shaft power meter has achieved a measurement accuracy of  $\pm 0.5\%FS$ , meeting the needs of most industrial applications, there is still room for further improvement in some special fields that require extremely high accuracy, such as aerospace and high-end precision manufacturing. Future research can start from optimizing sensor design, improving data processing algorithms, and enhancing the system's anti-interference ability. In sensor design, explore new sensor materials and structures to improve the sensitivity and stability of sensors and reduce measurement errors. Develop sensors based on new nanomaterials, utilizing the unique physical properties of nanomaterials to improve the detection accuracy of physical quantities related to shaft power. In terms of data processing algorithms, we will conduct in-depth research on more advanced data fusion algorithms and error correction algorithms, and combine artificial intelligence and machine learning technologies to process and analyze measurement data more accurately, further improving measurement accuracy. Using deep learning algorithms to train a large amount of measurement data, establish more accurate measurement models, and achieve automatic correction of measurement errors.

## Funding

2025 Zhejiang Province University Student Science and Technology Innovation Activity Plan (New Talent Plan) Project

## Data Availability

Data sharing is not applicable to this article as no new data were created or analysed in this study.

## Conflict of Interest

The author states that this article has no conflict of interest.

## References

- [1] IMO, *Resolution MEPC.328(76) amendments to the annex of the protocol of 1997 to amend the international convention for the prevention of pollution from SHIPS, 1973, as modified by the protocol of 1978 relating thereto.* [https://wwwcdn.imo.org/localresources/en/KnowledgeCentre/IndexofIMOResolutions/MEPCDocuments/MEPC.328\(76\).pdf](https://wwwcdn.imo.org/localresources/en/KnowledgeCentre/IndexofIMOResolutions/MEPCDocuments/MEPC.328(76).pdf), 2021. (Accessed 15 April 2024).
- [2] Korean Register, *CII Regulatory Response Guidelines (in Korean)*, 2021. [krs.co.kr/TECHNICAL\\_FILE/CII%20%EA%B7%9C%EC%A0%9C%20%EB%8C%80%EC%9D%91%20%EC%A7%80%EC%B9%A8%EC%84%9C\(October\).pdf](https://krs.co.kr/TECHNICAL_FILE/CII%20%EA%B7%9C%EC%A0%9C%20%EB%8C%80%EC%9D%91%20%EC%A7%80%EC%B9%A8%EC%84%9C(October).pdf). (Accessed 19 February 2024).
- [3] P. Balcombe, J. Brierley, C. Lewis, L. Skatvedt, J. Speirs, A. Hawkes, I. Staffell, *How to decarbonise international shipping: options for fuels, technologies and policies.* *Energy Convers, Manag* 182 (2019) 72–88, <https://doi.org/10.1016/j.enconman.2018.12.080>.

- [4]D.H. Kim, *CII status and improvement plan*, in: *Ship & Marine Design Research Society in the Society of Naval Architects of Korea, Changwon, Republic of Korea (23 February 2023)*, HD HYUNDAI HEAVY INDUSTRIES, 2023.
- [5]T.H. Kim, *Methanol as an alternative fuel*, in: *Ship & Marine Design Research Society in the Society of Naval Architects of Korea, Changwon, Republic of Korea (23 February 2023)*, HD HYUNDAI HEAVY INDUSTRIES, 2023.
- [6]E. Czermanski, A. Oniszczyk-Jastrzabek, E.F. Spangenberg, L. Kozłowski, M. Adamowicz, J. Jankiewicz, G.T. Cirella, *Implementation of the energy efficiency existing ship Index: an important but costly step towards ocean protection*, *Mar. Policy* 145 (105259) (2022), <https://doi.org/10.1016/j.marpol.2022.105259>.
- [7]Darko Gluji'c, Predrag Kralj, Josip Dujmovi'c, *Considerations on the effect of slowsteaming to reduce carbon dioxide emissions from ships*, *J. Mar. Sci. Eng.* 2022 (10) (2022) 1277, 10.3390/jmse10091277.
- [8]Mohamad Issa, Adrian Ilinca, Fahed Martini, *Ship energy efficiency and maritime sector initiatives to reduce carbon emissions*. *Energies*, 2022 15 (21) (2022) 7910, <https://doi.org/10.3390/en15217910>.
- [9]Statista, *Average speed of global merchant fleet by ship type 2018*. <https://www.statista.com/statistics/1268217/average-speed-of-ships-by-ship-type/>,2023.(Accessed 20 November 2023).
- [10]Kai Wang, Xiping Yan, Yupeng Yuan, Xiaoli Jiang, Xiao Lin, Rudy R. Negenborn, *Dynamic optimization of ship energy efficiency considering time-varying environmental factors*, *Transport. Res. Part D* 62 (2018) (2018) 685–698, <https://doi.org/10.1016/j.trd.2018.04.005>.
- [11]Mukesh Kumar, Bijan Kumar Mandal, Aritra Ganguly, Ravikant Ravi, Tabish Alam, Md Irfanul Haque Siddiqui, Sayed M. Eldin, *Performance evaluation of a diesel engine fueled with Chlorella Protothecoides microalgal biodiesel*, *Case Stud. Therm. Eng.* 51 (2023) (2023) 103609, <https://doi.org/10.1016/j.csite.2023.103609>.
- [12]Sunil Sharma, Naresh Kumar, Mohd Avesh, Rakesh Chandmal Sharma, Md Irfanul Haque Siddiqui, Jaesun Lee, *Navigating tranquillity with  $H_\infty$  controller to mitigate ship propeller shaft vibration*, *Journal of Vibration Engineering & Technologies* (2024),<https://doi.org/10.1007/s42417-024-01340-0>.
- [13]ClassNK Consulting Service, *Information on EEXI support services*. <https://www.classnkcs.co.jp/eexi/pdf/service-detail.pdf>, 2021. (Accessed 20 November 2023).